

Intratumoral heterogeneity of F-18 FDG uptake differentiates between gastrointestinal stromal tumors and abdominal malignant lymphomas on PET/CT

Tadashi Watabe · Mitsuaki Tatsumi · Hiroshi Watabe · Kayako Isohashi · Hiroki Kato · Masahiro Yanagawa · Eku Shimosegawa · Jun Hatazawa

Received: 10 October 2011 / Accepted: 23 November 2011 / Published online: 21 December 2011
© The Japanese Society of Nuclear Medicine 2011

Abstract

Objective Gastrointestinal stromal tumors (GISTs) and malignant lymphomas (MLs) in the abdomen are often observed as tumors of unknown origin on F-18 FDG PET/CT. The purpose of this study was to evaluate the intratumoral metabolic heterogeneity of F-18 FDG uptake on PET to determine if it might be helpful to discriminate between these tumors.

Methods The F-18 FDG PET/CT findings of 21 large abdominal tumors were retrospectively evaluated (9 GISTs and 12 MLs). Intratumoral heterogeneity was evaluated by

visual scoring (visual score: 0, homogeneous; 1, slightly heterogeneous; 2, moderately heterogeneous; 3, highly heterogeneous) and by the cumulative standardized uptake value (SUV) histograms on transaxial PET images at the maximal cross-sectional tumor diameter. Percent tumor areas above a threshold from 0 to 100% of the maximum SUV were plotted and the area under curve of the cumulative SUV histograms (AUC-CSH) was used as a heterogeneity index, where lower values corresponded with increased heterogeneity. Correlation between the visual score and the AUC-CSH was investigated by the Spearman's rank test.

Results GISTs exhibited heterogeneous uptake of F-18 FDG, whereas MLs showed rather homogeneous uptake on visual analysis (visual score: 2.67 ± 0.50 and 0.58 ± 0.79 , respectively; $p < 0.001$). The AUC-CSH was significantly lower for the GISTs than for the MLs (0.41 ± 0.14 and 0.64 ± 0.08 , respectively; $p < 0.001$). Significant correlations were observed between the visual score and the AUC-CSH ($\rho = -0.866$, $p < 0.001$).

Conclusion GISTs exhibited significantly heterogeneous intratumoral tracer uptake as compared with the MLs. Evaluation of the intratumoral heterogeneity of F-18 FDG uptake may help in the discrimination between these tumors.

T. Watabe · K. Isohashi · H. Kato · E. Shimosegawa · J. Hatazawa (✉)
Department of Nuclear Medicine and Tracer Kinetics,
Osaka University Graduate School of Medicine,
2-2 Yamadaoka, Suita, Osaka 565-0871, Japan
e-mail: hatazawa@tracer.med.osaka-u.ac.jp

T. Watabe · M. Tatsumi · K. Isohashi · H. Kato · M. Yanagawa · E. Shimosegawa · J. Hatazawa
Department of Nuclear Medicine, Osaka University Hospital,
2-2 Yamadaoka, Suita, Osaka 565-0871, Japan

T. Watabe · J. Hatazawa
Immunology Frontier Research Center, Osaka University,
2-2 Yamadaoka, Suita, Osaka 565-0871, Japan

M. Tatsumi
Department of Radiology, Osaka University Hospital,
2-2 Yamadaoka, Suita, Osaka 565-0871, Japan

H. Watabe
Department of Molecular Imaging in Medicine,
Osaka University Graduate School of Medicine, Suita, Japan

M. Yanagawa
Department of Radiology,
Osaka University Graduate School of Medicine, Suita, Japan

Keywords F-18 FDG PET · Intratumoral heterogeneity · Gastrointestinal stromal tumor · Malignant lymphoma · Cumulative standardized uptake value histograms

Introduction

Gastrointestinal stromal tumors (GISTs) and malignant lymphomas (MLs) in the abdomen are often observed as tumors of unknown origin on F-18 fluorodeoxyglucose (FDG) PET/CT examinations. Characteristics of tumors are

often determined by the intensity of F-18 FDG uptake, usually by the maximum standardized uptake value (SUV_{max}). SUV_{max} is calculated based on the hottest uptake of the tumor and does not reflect the activity throughout the tumor. Heterogeneous F-18 FDG uptake is sometimes encountered in large abdominal tumors. For example, GISTs often exhibit heterogeneous uptake as compared with other types of tumors, even if the SUV_{max} is on the same level. On the other hand, homogeneous uptake has often been observed in MLs. Thus, evaluation of the intratumoral heterogeneity of F-18 FDG uptake may provide us with additional information about the tumor characteristics. A recent study reported that the detection of intratumoral metabolic heterogeneity on baseline F-18 FDG-PET is useful for predicting the response to concomitant radiochemotherapy in esophageal cancer [1]. However, no study has reported evaluation of the intratumoral distribution of F-18 FDG on PET to differentiate among tumors of unknown origin. Intratumoral metabolic activity is not uniform and may differ depending on the characteristics of the tumor cells such as the cellular proliferative activity and the state of the microenvironment such as presence/absence of hypoxia [2]. We evaluated the intratumoral heterogeneity of F-18 FDG uptake on PET, which was considered to reflect the tumor characteristics. The purpose of this study was to evaluate the intratumoral metabolic heterogeneity in GISTs and MLs on PET images to determine if it might be helpful in discriminating between these two types of tumors.

Materials and methods

Patients

Twenty-one patients with abdominal tumors were retrospectively evaluated in this study. All patients were examined by F-18 FDG PET/CT before treatment from

June 2007 to October 2010 at our hospital. Inclusion criteria of the patients were as follows: (1) abdominal tumors measuring more than 5 cm in the major-axis maximal diameter and (2) finally diagnosed as GISTs or MLs by histopathological examination of biopsy or surgical specimens. The characteristics of the two groups of the patients (GIST group: $n = 9$; ML group: $n = 12$) and extent of the lesions are summarized in Table 1. The histological diagnoses in the ML group included diffuse large B-cell lymphoma (DLBCL) and follicular lymphoma (FL). The clinical staging in the ML group was performed according to the Ann Arbor classification. This study was approved by the Ethics Committee of the Osaka University Hospital.

PET

After at least 4 h of fasting, the patients received an intravenous injection of F-18 FDG (approximately 3.7 MBq (0.1 mCi)/kg body weight). PET/CT exams were performed about 60 min after the administration of F-18 FDG. Imaging was performed with an integrated PET/CT scanner (GEMINI GXL, Philips). Whole-body images were acquired generally from the top of the skull to the mid-thighs. PET images were acquired under the following acquisition conditions: 3D emission scan, 2 min scan/bed position \times 9–11 positions, and 4.0-mm slice thickness/interval. The PET images were reconstructed with the 3-dimensional (3D) line-of-response row-action maximum-likelihood algorithm using standard protocol parameters (relaxation parameter of 0.04). The spatial resolutions at the center of the PET were 5.2 mm full width at half maximum (FWHM) in the transaxial direction and 6.0 mm FWHM in the axial direction. The acquisition conditions for the CT (16-slice CT) were as follows: breathhold during normal expiration from the level of the lung apex to the lower poles of the kidneys, without intravenous or oral contrast medium, 120 kVp and 50 effective mAs,

Table 1 Characteristics of the patients and extent of the lesions

	GIST	ML
Total number	9	12
Age (years)	58.1 \pm 13.6	59.2 \pm 10.8
Sex (male/female)	5/4	4/8
Recurrent tumor	4	2
GIST ($n = 9$)		
Primary site	Gastric 3, small intestine 3, peritoneum 2, unknown 1	
Metastasis	Liver 3, peritoneum 3, both liver and peritoneum 1	
ML ($n = 12$)		
Histology	Non-Hodgkin's lymphoma (diffuse large B-cell type 6, follicular type 6)	
Stage (Ann Arbor)	I: 1, II: 2, III: 6, IV: 3	

5.0-mm slice thickness/4.0 mm interval. The CT scan data were used for the attenuation correction as well as image fusion. The matrix size was 144×144 (4 mm \times 4 mm for each pixel) for PET and 512×512 (1.17 mm \times 1.17 mm for each pixel) for CT.

Data analysis

Single tumor lesion (primary site in GISTs or the largest lymph node in MLs) was selected in each patient and transaxial PET image at the maximal cross-sectional tumor diameter was used for evaluation of the intratumoral metabolic heterogeneity. Visual assessment was performed by two experienced nuclear medicine physicians who were unaware of the patients' histories or diagnosis, using a visual scoring system, as follows: 0, homogeneous uptake; 1, slight heterogeneous uptake; 2, moderate heterogeneous uptake; 3, highly heterogeneous uptake. The decision on the visual score was based on the consensus of the two observers.

SUV was used for the semi-quantitative evaluation of the PET images. A two-dimensional region-of-interest (2D-ROI: range 9.7–334.7 cm²) was manually drawn on the tumor area of the transaxial PET images. Definition of the tumor area was based on the CT image with reference to the fused PET/CT images. The SUV_{max} of the 2D-ROI (2D-SUV_{max}) and that of the whole tumor (3D-SUV_{max}) were measured from the PET image. Intratumoral heterogeneity of uptake was evaluated by the simple method of the coefficient of variation (CV) in the 2D-ROIs, which was calculated as the standard deviation (SD) of the SUV divided by the mean SUV. The F-18 FDG PET threshold tumor area was calculated to draw cumulative SUV histograms (CSH). CSH was reported to be a novel way to characterize heterogeneity in intratumoral tracer uptake [3]. CSH is obtained by plotting the percent area of tumor with an SUV above a certain threshold against that threshold, which is varied from 0 to 100% of the SUV_{max}. The AUC of this plot (AUC-CSH) is a quantitative index of uptake heterogeneity, where lower values correspond with increased heterogeneity. The percent threshold tumor areas were calculated by Osirix software (32 bit, version 3.8.1) and ImageJ software (1.43u) (Fig. 1). The correlations among the visual score, 2D-SUV_{max}, CV, AUC-CSH, and tumor area were also investigated.

Statistical analysis

The data between the two groups were compared by Mann–Whitney's test. Correlation between the visual score and other parameters were assessed by calculation of the Spearman's rank correlation coefficient. Probability values of less than 0.05 were considered to denote statistical significance.

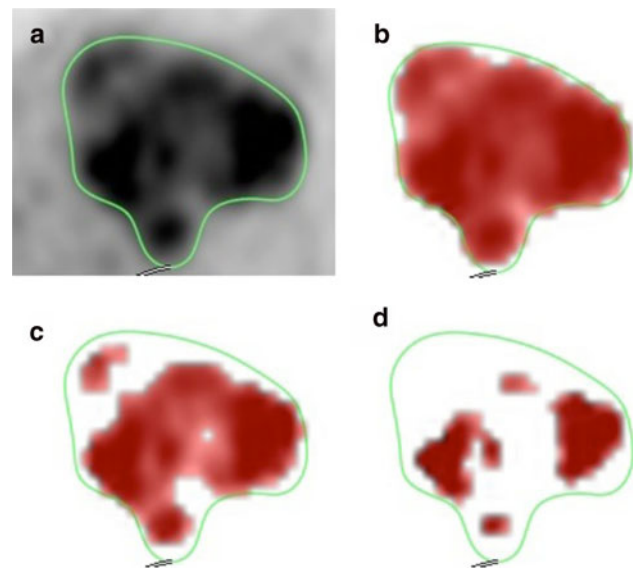


Fig. 1 a 2D-ROI area and threshold tumor area showing over b 30, c 50, and d 70% of the 2D-SUV_{max}. (percent area = 98.3, 68.5, and 28.6%, respectively)

Results

PET images in the GIST group exhibited heterogeneous distribution of F-18 FDG uptake, whereas the ML group showed a rather homogeneous pattern on visual analysis (visual score: 2.67 ± 0.50 and 0.58 ± 0.79 , respectively, $p < 0.001$). Representative images from the two groups are shown in Figs. 2 and 3.

The results of ROI analysis are shown in Table 2; the CV was significantly higher in the GIST group than in the ML group (0.58 ± 0.30 and 0.31 ± 0.09 , respectively, $p = 0.001$). The AUC-CSH were significantly lower in the GIST group than in the ML group (0.41 ± 0.14 and 0.64 ± 0.08 , respectively, $p = 0.001$), which suggested that the F-18 FDG uptake in the GISTs was more heterogeneous than that in the MLs. Changes of the AUC-CSH in every patient of both groups are shown in Fig. 4, which represented the different curves between the GISTs and MLs. The visual score was significantly correlated with the CV, the tumor area, and the AUC-CSH (Table 3).

The comparison between DLBCLs and FLs are shown in Table 4. DLBCLs showed higher 3D-SUV_{max} than FLs (17.0 ± 5.9 and 8.3 ± 0.8 , respectively). However, the differences of the visual score and the intratumoral heterogeneity index (the CV and the AUC-CSH) between the DLBCLs and FLs were small and not statistically significant.

Discussion

GISTs are mesenchymal neoplasms with a spectrum of histologic appearances and biologic activity [4] and arise

Fig. 2 **a** PET/CT, **b** CT, **c** PET image, and **d** 3D-histogram on tumor in a 38-year-old male patient with GIST. Transaxial PET/CT image (**a, b**) shows a huge mass lesion in the pelvic cavity (*arrow*); axial PET image (**c**) shows a heterogeneous distribution of FDG ($2D-SUV_{max} = 6.5$). 3D-histogram (**d** inside the square on the PET image) shows heterogeneous uptake

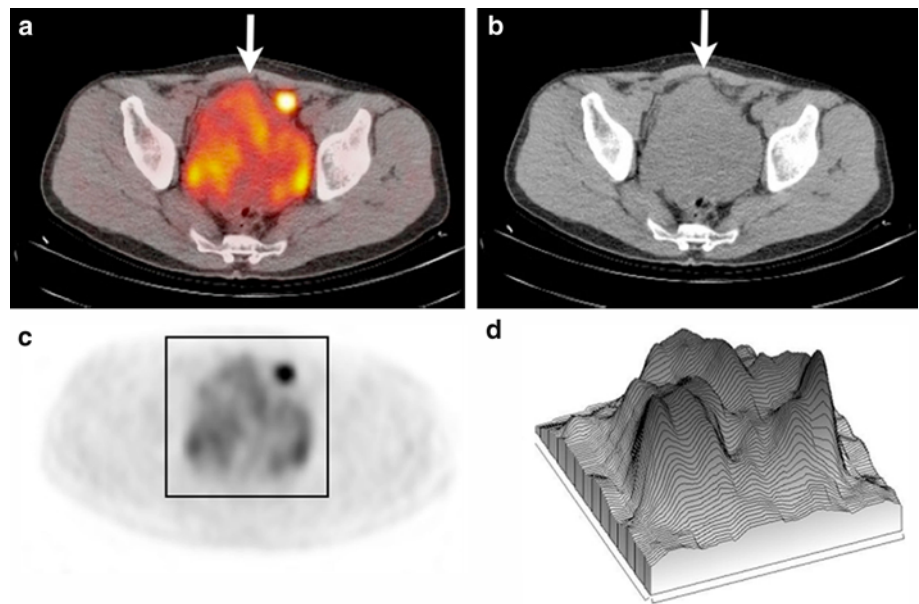
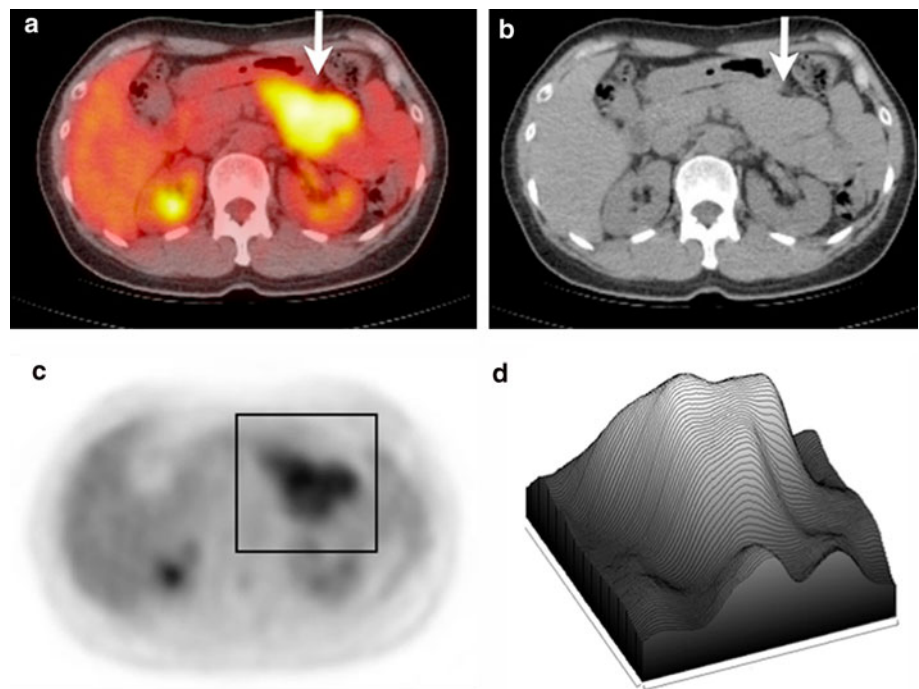


Fig. 3 **a** PET/CT, **b** CT, **c** PET image, and **d** 3D-histogram of a tumor in a 54-year-old female patient with ML (FL). Transaxial PET/CT image (**a, b**) shows a mass lesion between the stomach and left kidney (*arrow*); the transaxial PET image **c** shows a rather homogeneous distribution of F-18 FDG ($2D-SUV_{max} = 7.2$); 3D-histogram (**d** inside the square on the PET image) shows a relatively smooth and uniform uptake



from anywhere in the gastrointestinal tract (from the esophagus to the rectum) [5]. It has been reported that F-18 FDG PET is useful for evaluating the therapeutic responses of these tumors to drugs, such as imatinib [6]. We evaluated the intratumoral heterogeneity of F-18 FDG uptake to discriminate them from other abdominal tumors for diagnosis. A previous study reported heterogeneous enhancement in large GISTs on enhanced CT [7]. Focal areas of low attenuation on CT in small GISTs represent varying pathological conditions, including solid tumor, hemorrhage, hemorrhage with necrosis, cystic degeneration, fluid

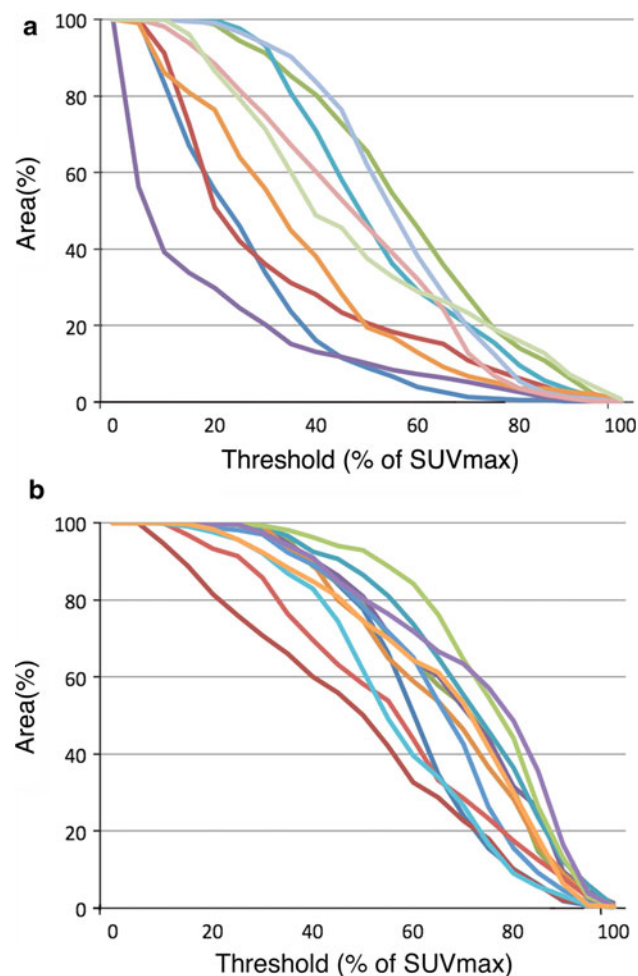
in ulcers, and fibrous septum [8]. Large GISTs (>6 cm) frequently show central areas of necrosis or hemorrhage, resulting in a cystic appearance [4, 9]. In our study, areas of lower F-18 FDG uptake in GISTs often corresponded to the low-attenuation areas on CT and were considered to reflect the aforementioned pathological features. However, heterogeneous F-18 FDG uptake was observed in solid portions of the GISTs, which corresponded to areas of homogeneous density on CT.

MLs are malignant neoplasms composed of monoclonal proliferations of lymphocytes derived from either B cells or

Table 2 Results of visual and ROI analysis of the GIST and ML groups

	GIST	ML	<i>p</i> value
Visual score	2.67 ± 0.50	0.58 ± 0.79	<0.001*
2D-SUV _{max}	7.4 ± 2.6	11.0 ± 6.4	0.219
3D-SUV _{max}	9.0 ± 3.6	12.6 ± 6.0	0.169
CV	0.58 ± 0.30	0.31 ± 0.09	0.001*
AUC-CSH	0.41 ± 0.14	0.64 ± 0.08	0.001*
Tumor area (cm ²)	118.6 ± 102.1	40.1 ± 31.6	0.034 [†]

Mean ± SD

* *p* < 0.01, [†] *p* < 0.05**Fig. 4** CSH in the GIST and ML groups (a GISTs, b MLs)

T cells at various stages of their differentiation [10]. The molecular characteristics and biologic behavior of these tumors differ according to the histologic subtype. MLs can be divided into aggressive and indolent types according to the clinical course. The ML subtypes included in our study were FL (indolent type) and DLBCL (aggressive type). On CT images, MLs typically show homogeneous attenuation

Table 3 Correlation between the visual score and other parameters

	Coefficient of correlation	<i>p</i> value
CV	0.726	<0.001*
AUC-CSH	−0.866	<0.001*
2D-SUV _{max}	−0.151	0.513
Tumor area (cm ²)	0.518	0.016 [†]

* *p* < 0.01, [†] *p* < 0.05**Table 4** Results of visual and ROI analysis in the DLBCL and FL groups

	DLBCL	FL	<i>p</i> value
Visual score	1.00 ± 0.89	0.17 ± 0.41	0.132
2D-SUV _{max}	15.0 ± 7.1	7.0 ± 0.7	0.065
3D-SUV _{max}	17.0 ± 5.9	8.3 ± 0.8	0.041 [†]
CV	0.36 ± 0.10	0.27 ± 0.04	0.132
AUC-CSH	0.60 ± 0.08	0.68 ± 0.04	0.093
Tumor area (cm ²)	51.9 ± 39.8	28.3 ± 16.6	0.240

Mean ± SD

[†] *p* < 0.05

on non-contrast images, related to the inherent hypercellularity of the lymphoma masses [11]. Intratumoral necrosis is rarely seen before chemotherapy. In our study, both FLs and DLBCLs exhibited a homogeneous density on CT, without any areas of low attenuation.

FLs generally show low-to-moderate F-18 FDG uptake on PET [12]. Typical FL accounts for most cases of low-grade FLs and represents a homogeneous disease entity with definitive morphological characteristics, phenotype, and gene aberrations [13]. DLBCLs generally exhibit marked elevation of F-18 FDG uptake on PET/CT [14]. In our study, DLBCLs showed markedly high uptake and FLs had moderate uptake, which corresponded to the previous study.

In many previous F-18 FDG PET studies, the tumor characteristics were usually evaluated by the 3D-SUV_{max}, which reflected only a single voxel with the maximum uptake, and few PET studies have focused on the intratumoral distribution of F-18 FDG [1, 3, 15]. The CSH method that we applied in our study was recently reported for parameterizing heterogeneous intratumoral F-18 FDG uptake in non-small cell lung cancer PET studies [3]. This method can be applied for 2D-ROI analysis to evaluate large tumors. The heterogeneity of F-18 FDG uptake may be greatly affected by the tumor size and spatial resolution of PET. Our inclusion criteria of the tumor were measuring more than 5 cm in the major-axis maximal diameter, which is approximately 10 times as large as FWHM in the transaxial direction. Therefore, tumor size was large enough to evaluate by the transaxial PET slice at the

maximal diameter as a representative image of the entire tumor.

The results of visual scoring evaluation were significantly correlated with the AUC-CSH, which showed the better correlation than the CV. Our evaluation by visual analysis corresponded to the quantitative method to characterize the intratumoral metabolic heterogeneity.

There were no significant correlations between the visual score and the 2D-SUV_{max}, which suggested that the 2D-SUV_{max} does not reflect the intratumoral metabolic heterogeneity, although higher 2D-SUV_{max} may be associated with a greater likelihood of metabolic heterogeneity. In our study, DLBCLs, which showed the highest 2D-SUV_{max}, showed homogeneous uptake as compared with GISTs. F-18 FDG PET evaluation revealed that while FLs and GISTs were on the similar 2D-SUV_{max} levels, they exhibited significant differences in intratumoral heterogeneity of F-18 FDG uptake.

The limitations of our study was that we did not account for the difference in the tumor volume between the GISTs and MLs; the GISTs showed a higher average tumor volume than the MLs. In general, larger tumors may be expected to show more heterogeneous F-18 FDG uptake on PET. In our study, the visual score was significantly correlated with the tumor area, which suggested that tumor volume might be one of the major determinants of intratumoral metabolic heterogeneity.

Conclusion

In this F-18 FDG PET/CT study, GISTs exhibited significantly more heterogeneous intratumoral uptake as compared with MLs. We used a 2D-ROI analysis method for evaluating the intratumoral tracer distribution, the results of which showed a good correlation with the results of the visual assessment. Evaluation of the intratumoral metabolic heterogeneity on F-18 FDG PET images may help discriminate between these tumors.

Acknowledgments The authors thank the staff of the Department of Nuclear Medicine, Osaka University Hospital, for their excellent technical assistance.

Conflict of interest The authors declare that they have no conflict of interest and no source of funding.

References

1. Tixier F, Le Rest CC, Hatt M, Albarghach N, Pradier O, Metges JP, et al. Intratumor heterogeneity characterized by textural features on baseline 18F-FDG PET images predicts response to concomitant radiochemotherapy in esophageal cancer. *J Nucl Med*. 2011;52:369–78.
2. Pugachev A, Ruan S, Carlin S, Larson SM, Campa J, Ling CC, et al. Dependence of FDG uptake on tumor microenvironment. *Int J Radiat Oncol Biol Phys*. 2005;62:545–53.
3. van Velden FH, Cheebsumon P, Yaqub M, Smit EF, Hoekstra OS, Lammertsma AA, et al. Evaluation of a cumulative SUV-volume histogram method for parameterizing heterogeneous intratumoural FDG uptake in non-small cell lung cancer PET studies. *Eur J Nucl Med Mol Imaging*. 2011;38:1636–47.
4. Laurini JA, Carter JE. Gastrointestinal stromal tumors: a review of the literature. *Arch Pathol Lab Med*. 2010;134:134–41.
5. Kochhar R, Manoharan P, Leahy M, Taylor MB. Imaging in gastrointestinal stromal tumours: current status and future directions. *Clin Radiol*. 2010;65:584–92.
6. Basu S, Mohandas KM, Peshwe H, Asopa R, Vyawahare M. FDG-PET and PET/CT in the clinical management of gastrointestinal stromal tumor. *Nucl Med Commun*. 2008;29:1026–39.
7. Lau S, Tam KF, Kam CK, Lui CY, Siu CW, Lam HS, et al. Imaging of gastrointestinal stromal tumour (GIST). *Clin Radiol*. 2004;59:487–98.
8. Kim HC, Lee JM, Kim SH, Park SH, Lee JW, Lee M, et al. Small gastrointestinal stromal tumours with focal areas of low attenuation on CT: pathological correlation. *Clin Radiol*. 2005;60:384–8.
9. Chourmouzi D, Sinakos E, Papatavrentios L, Akriviadis E, Drevelegas A. Gastrointestinal stromal tumors: a pictorial review. *J Gastrointest Liver Dis*. 2009;18:379–83.
10. Coupland SE. The challenge of the microenvironment in B-cell lymphomas. *Histopathology*. 2011;58:69–80.
11. Anis M, Irshad A. Imaging of abdominal lymphoma. *Radiol Clin North Am*. 2008;46:265–85.
12. Allen-Auerbach M, de Vos S, Czernin J. The impact of fluorodeoxyglucose-positron emission tomography in primary staging and patient management in lymphoma patients. *Radiol Clin North Am*. 2008;46:199–211.
13. Guo Y, Karube K, Kawano R, Yamaguchi T, Suzumiya J, Huang GS, et al. Low-grade follicular lymphoma with t(14;18) presents a homogeneous disease entity otherwise the rest comprises minor groups of heterogeneous disease entities with Bcl2 amplification, Bcl6 translocation or other gene aberrances. *Leukemia*. 2005;19:1058–63.
14. Schoder H, Noy A, Gonen M, Weng L, Green D, Erdi YE, et al. Intensity of ¹⁸F-fluorodeoxyglucose uptake in positron emission tomography distinguishes between indolent and aggressive non-Hodgkin's lymphoma. *J Clin Oncol*. 2005;23:4643–51.
15. O'Sullivan F, Roy S, Eary J. A statistical measure of tissue heterogeneity with application to 3D PET sarcoma data. *Biostatistics*. 2003;4:433–48.